**Title:** Improving emotion control in social anxiety by targeting rhythmic brain circuits

**Abbreviated title:** Improving emotional action control in social anxiety

**Authors:** Sjoerd Meijer[1†*], Bob Bramson[1,2†], Ivan Toni[1‡], and Karin Roelofs[1,2‡]

**Affiliations:** [1]*Donders Institute for Brain, Cognition and Behavior, Centre for Cognitive Neuroimaging (DCCN), Radboud University Nijmegen, 6525 EN Nijmegen, the Netherlands.* [2]*Behavioral Science Institute (BSI), Radboud University Nijmegen, 6525 GD Nijmegen, the Netherlands.*

[*]Corresponding author. E-mail: sjoerd.meijer@donders.ru.nl

[†,‡]These authors contributed equally to this work.

**Manuscript pages:** 29

**Figures:** 3

**Tables:** 1

**Wordcount:** Abstract (158), Introduction (477), Discussion (1239)

**Key words:** social anxiety; emotion control; approach-avoidance behavior; phase-amplitude coupling; transcranial electrical brain stimulation

**Competing interests:** The authors declare that they have no competing interests.

**Acknowledgments:** We thank Jesse Lam for his support with data collection.

**Funding:** This work was funded by a consolidator grant DARE2APPROACH, from the European Research Council (ERC_CoG_772337) awarded to KR and also supporting SM and BB; by a consortium grant from the Dutch Research Council INTENSE (NWO_Crossover_17619) and by (NWO_SSH_406.20.GO.020) awarded to IT and KR.

**Data and materials availability:** All behavioral and fMRI data, along with the analysis scripts, will be made available at https://doi.org/10.34973/jjjq-nr84.

**ABSTRACT** (158/250)

Social avoidance is a hallmark of social anxiety disorder. Difficulties in controlling avoidance behavior are the core maintaining factor of this impairing condition, hampering the efficacy of existing therapies. This preregistered study tested a physiologically-grounded non-invasive enhancement of control over social approach and avoidance behavior in socially anxious individuals. Their prefrontal and sensorimotor areas received dual-site phase-coupled electrical stimulation, to enhance endogenous inter-regional theta-gamma phase-amplitude coupling, a mechanism known to support emotion control in non-anxious individuals. We measured behavioral and fMRI-BOLD responses during in-phase, anti-phase, and sham stimulations, while participants performed a social approach-avoidance task, involving either automatic or controlled emotional actions. In-phase stimulation selectively enhanced control over approach-avoidance actions, and modulated neural responses in the same prefrontal region where stimulation-reactivity increased as a function of trait anxiety. These findings illustrate how human neurophysiological connectivity can be leveraged to improve control over social avoidance, opening the way for mechanistically grounded clinical interventions of persistent avoidance in anxiety disorders.

**SIGNIFICANCE STATEMENT** (107/120)

Controlling automatic approach-avoid behavior is essential for human social interactions. This ability is impaired in social anxiety, but we know how neurotypical brains use endogenous rhythmic coupling for social emotion control. In a preregistered study, we used noninvasive electrical brain stimulation to enhance endogenous rhythmic coupling between prefrontal theta- and sensorimotor gamma-band rhythms, while highly socially anxious individuals solved an emotional control challenge. In-phase stimulation selectively enhanced emotional action control and modulated neural activity in a prefrontal cortex region where brain stimulation reactivity increased as a function of trait anxiety. These findings provide evidence for the generalizability and clinical potential of this interventional approach to social anxiety.

## **INTRODUCTION** (477/650)

Anxiety disorders are marked by an inability to flexibly regulate prepotent approach and avoidance tendencies to adapt behavior to contextual demands. Persistent avoidance of perceived threats causes and maintains anxiety, preventing the extinction of those threats through exposure, thereby exacerbating the disorder (Lovibond et al., 2009; Pittig et al., 2015; Craske and Stein, 2016; Rattel et al., 2017). There is an urgent need for non-invasive interventions targeted at improving emotional action control in anxious individuals. Recent work has improved cognitive and behavioral functions in neurotypical individuals, boosting inter-regional neural communication through dual-site phase-amplitude-coupled transcranial alternating current stimulation (dual-site tACS) (Polanía et al., 2012; Violante et al., 2017; Preisig et al., 2021; Grover et al., 2022). This non-invasive neuromodulation technique, grounded on the physiology of directional inter-regional neuronal communication, can also enhance emotion control in non-anxious individuals (Bramson et al., 2020a). Here, we test the generalizability of this approach by applying dual-site tACS in a group of participants selected for high social anxiety, a trait known to be associated with impaired emotional action control (Heuer et al., 2007; Roelofs et al., 2009b; van Peer et al., 2009). This translational test is a critical step toward developing clinically-relevant interventions for modulating emotional behavioral control.

Patients suffering from social anxiety disorder have particular difficulties in overriding automatic avoidance tendencies in social situations. Previous research has identified the lateral prefrontal cortex (lPFC) as a critical brain region involved in selecting between competing approach-avoidance actions (Koch et al., 2018; Bramson et al., 2020b). This control is implemented through rhythmic modulation of excitability in downstream areas, including the sensorimotor cortex (SMC) and parietal cortex (Voytek et al., 2015; Bramson et al., 2018, 2020a; Weber et al., 2024). Specifically, successful control over social-emotional approach-avoidance actions has been linked to coupling between the phase of theta-band rhythms in lPFC and the amplitude of gamma-band activity in SMC (Voytek et al., 2015; Bramson et al., 2018; Weber et al., 2024).

Dual-site tACS offers a means to non-invasively modulate endogenous inter-regional phase-amplitude coupling, enhancing long-range synchronization between task-relevant neural circuits (Reinhart and Nguyen, 2019; Bramson et al., 2020a; Grover et al., 2022). Our work has shown that in-phase stimulation, designed to synchronize peaks of theta-band rhythms in lPFC with the amplitude of gamma-band neural activity in SMC, improves accuracy when non-anxious

participants override automatic emotional action tendencies (Bramson et al., 2020a). Given the pivotal role of the lPFC in regulating approach-avoidance actions (Volman et al., 2011) and the importance of theta-gamma coupling between lPFC and SMC for successful control over social-emotional approach-avoidance actions (Bramson et al., 2018, 2020a), here we test whether dual-site tACS applied to lPFC-SMC can enhance emotional action control in highly socially anxious individuals. We applied in-phase and anti-phase dual-site tACS while forty-nine highly socially anxious individuals performed an approach-avoidance task, using concurrent fMRI to quantify prefrontal engagement during control over emotional action tendencies.

## MATERIALS AND METHODS

### Participants

Fifty-two highly socially anxious students (39 females) from Radboud University, Nijmegen, were recruited to participate in this pre-registered experiment (https://osf.io/j9s2z/). The local ethics committee approved the experiment (METC Arnhem-Nijmegen: CMO2014/288). Two participants were excluded due to malfunctioning of the stimulation equipment, and one participant was excluded for failing to comply with task instructions during one of the stimulation sessions. Participants were selected based on high self-reported social anxiety levels, as detailed below, and screened for eligibility criteria, including no history of mental illness other than anxiety disorders or current use of psychoactive medication. Additionally, all participants had normal or corrected-to-normal vision and underwent screening for contraindications to magnetic resonance imaging (MRI) and non-invasive transcranial electrical stimulation. The mean age of participants was 24.0 years (SD = ±4.3), with an age range of 19 to 40 years.

Pre-screening was conducted using the Liebowitz Social Anxiety Scale (LSAS). Participants who scored 30 or higher (on the combined fear/anxiety and avoidance sub-scales) were included, as this cutoff provides an optimal balance between sensitivity and specificity for identifying individuals who meet the criteria for social anxiety disorder (Mennin et al., 2002). This selection criterion resulted in a normal distribution of LSAS scores within our study sample, with a mean of 64.4, a standard deviation (SD) of ±18.8, and a range from 31 to 106 (**Fig. 1A**). The trait sub-scale of the State-Trait Anxiety Inventory (STAI Y-2) was also included to assess trait anxiety, serving as an inter-individual difference marker of tACS BOLD dose-response. This is because endogenous prefrontal activation in response to the emotional action control challenge varies as a function of trait anxiety (Bramson et al., 2023).

The current study in highly socially anxious individuals was powered to replicate the main finding of our previous investigation in healthy male students (Bramson et al., 2020a) that showed tACS phase- and dose-specific effects on emotional action control (https://osf.io/j9s2z/). This required a sample size that allowed us to detect the previously observed significant three-way interaction between Congruency (congruent, incongruent) * tACS-phase (in-phase, anti-phase) * tACS-dose (BOLD signal in lPFC during stimulation *vs*. sham): $\eta_p^2 = 0.19$ (Bramson et al., 2020a). The minimum sample size required for this study to detect an effect of comparable magnitude is 45 participants (*a priori* sensitivity power analysis of 2x2 RM-ANCOVA: $\alpha = .05$, power = .80, $\eta_p^2 =$

0.19; G*Power v3.1(Faul et al., 2007)). Given that the current sample might be more heterogeneous due to mixed-sex and anxiety-related differences, we decided to increase our planned sample size to 50 participants.

**Procedure**

The data collection procedure took place over three separate days. On the first day, participants completed the Liebowitz Social Anxiety Scale (LSAS) and State-Trait Anxiety Inventory-Trait (STAI-trait, Y-2) questionnaires. Following this, participants underwent a series of scanning procedures, including a structural T1-weighted scan, a diffusion-weighted imaging scan (DWI, as reported in (Bramson et al., 2020a, 2023)), and a magnetic spectroscopy scan (MRS, as reported in (Bramson et al., 2020a, 2023)).

On the second and third days of the experiment, neuronavigation was employed to position the electrodes over the sensorimotor cortex (SMC) and lateral prefrontal cortex (lPFC). Detailed information on electrode placement is provided in the following section. During both stimulation sessions, participants were positioned inside the MR scanner, where they first completed a 5-minute practice task. After the practice session, participants proceeded with the approach-avoidance task, which was conducted concurrently with dual-site tACS intervention and task-based functional MRI for approximately 35 minutes.

**Approach-avoidance task**

Emotional action control was manipulated using a validated social approach-avoidance task in which cognitive control is associated with lPFC-SMC theta-gamma coupling (Bramson et al., 2018), and is sensitive to the phase-dependent effects of dual-site theta-gamma phase-amplitude tACS when controlling for inter-individual variation in prefrontal BOLD response to tACS (Bramson et al., 2020a). During functional MR scanning, participants lay inside the MR scanner with a joystick in their right hand resting on their lower abdomen. Participants were instructed to approach or avoid by moving the joystick toward or away from themselves, respectively. During the task, participants received written instructions on the screen (>10 s) at the start of each block of 12 trials (~60 s) that stated, *"Pull the joystick toward yourself when you see a happy face and push away from yourself when you see an angry face"* (congruent condition), *"Push the joystick away from yourself when you see a happy face and pull toward yourself when you see an angry face"* (incongruent condition). Congruent and incongruent conditions alternated between blocks in a pseudo-random fashion. Between blocks, there was an inter-block interval of >20 s. Each trial

started with a fixation cross (500 ms) followed by a face stimulus (100 ms) to which participants had to respond within 2 s. Joystick movements over 30% of the maximum movement range were considered valid responses. If a participant did not respond, they would receive on-screen feedback stating, *"You did not move the joystick far enough"*. Instructions and the inter-block interval lead to an ~30 s wash-out period between stimulation conditions. Each participant had 288 trials on each of the two testing days, yielding 576 observations (trials) in total, equally distributed over congruency (congruent, incongruent) and stimulation (in-phase, anti-phase, sham) condition combinations (96 trials per bin).

**Dual-site tACS stimulation**

Dual-site tACS was applied online during task performance inside the MRI scanner using two sets of concentric ring electrodes (inner disc: 25 mm ø; outer ring: 80 mm inner-ø, 100 mm outer-ø) (Saturnino et al., 2017). Current direction alternated (-1 mA to +1 mA) between each disc-ring electrode set to achieve a time-varying electrical field in theta-band (6 Hz) frequency over right-lPFC and gamma-band (75 Hz) tapered with a 6 Hz theta wave over left-SMC. The tACS-phase manipulation was achieved by phase-locking gamma-band power to peaks (in-phase) or troughs (anti-phase) of the theta-band signal. During sham blocks, there was an initial 10 s period of stimulation to match potential sensations related to the onset of stimulation, after which stimulation was terminated. Within a session, participants received all stimulation conditions (in-phase, anti-phase, sham) alternating in a pseudo-random fashion between stimulus blocks of 12 trials (~60 s), interleaved with periods of no stimulation (instructions between blocks; > 30 s), and never repeating the same stimulation condition for two consecutive blocks.

We used neuronavigation (Localite TMS Navigator; RRID: SCR_016126) for individualized targeting of left-SMC (MNI [-28, -32, 64] (Bramson et al., 2018, 2020a)) and right-lPFC (MNI [26, 54, 0] (Neubert et al., 2014; Bramson et al., 2018, 2020a)) based on anatomical masks of regions of interest registered to individual T1-weighted scans acquired during the first session. After localization, electrodes were attached to the participant's scalp using Ten20 conductive paste (MedCaT). Inside the MR scanner, stimulation was delivered using two Neuroconn DC-Stimulator Plus stimulators (neuroConn; impedance < 10 kOhm; RRID: SCR_015520). Stimulators were placed inside a magnetically shielded box designed with electronics that filtered out RF pulses of the MR scanner and combined with a BrainAmp ExG MR amplifier (www.brainproducts.com) that allowed continuous monitoring of stimulation output during the session.

208

209 **Modeling of stimulation currents**

210 The electric field magnitude (mV/mm) at the cortical target sites was estimated using SimNIBS
211 (version 4.0; (Thielscher et al., 2015)). The concentric ring electrode sets were modeled as the disc
212 (25 mm ø) and outer ring electrode (80 mm inner-ø, 100 mm outer-ø) with the same center, using
213 a 2-layer medium (2 mm silicone rubber on top of 2 mm saline gel). The electrode sets were
214 positioned over lPFC and SMC using the template head mesh of SimNIBS. For all media, we used
215 standard conductivities provided by SimNIBS. Direct currents of 1 mA were modeled to flow
216 between the center disc electrode and the outer ring. The model results of the electric field
217 magnitude at the cortical surface for both target sites are shown in **Fig. 2A**.

218

219 **MRI**

220 All participants underwent magnetic resonance imaging using a 3T MAGNETRON Prisma MR
221 scanner (Siemens AG, Healthcare Sector, Erlangen, Germany), which has a 64-channel head coil
222 with a top opening that allows the tACS electrode wires to be routed out of the back of the scanner
223 bore. The scans obtained during the MR sessions were aligned with a standard brain atlas to
224 guarantee a uniform field of view (FoV) throughout the days. Each scanning day involved taking
225 around 1800 functional images using a multi-band six sequence, 2 mm isotropic voxel size, TR/TE
226 = 1000 / 34 ms, flip angle = 60°, phase angle P >> A, including ten volumes with reversed phase
227 encoding direction (A >> P) used to correct image distortions.

228

229 High-resolution structural images were acquired with a single-shot MPRAGE sequence
230 using a GRAPPA acceleration factor of 2, TR/TE = 2400/2.13 ms, an effective voxel size of 1 mm
231 isotropic, 176 sagittal slices, a distance factor of 50%, a flip angle of 8°, orientation A >> P, and a
232 FoV of 256 mm.

233

234 **Behavior analyses**

235 To examine effects of congruency (congruent, incongruent) and stimulation (in-phase, anti-phase,
236 sham) on behavioral response accuracy (correct, incorrect), we employed mixed-effects logistic
237 regression using the *lme4* package in R (Bates et al., 2015). The models accounted for inter-
238 individual variability by incorporating random slopes, intercepts, and correlations across
239 participants to adhere to the maximal random effects structure. Outputs of these models are log
240 odds ('*b*'). Effect sizes were reported as odds ratios (ORs) with 95% confidence intervals (CIs).
241 Statistical significance for all analyses were evaluated at the $\alpha < 0.05$ criterion.

Mixed-effects logistic regression models included behavioral accuracy (correct, incorrect) as dependent variable, with the relevant experimental conditions (congruency, stimulation) and their interactions as predictors. The tACS-dose (see below; continuous variable; *Z*-scored) metric was added as covariate to the interaction.

We hypothesized that the congruency effect in error rates would decrease for in-phase tACS and that the size of the effect per participant would depend on the BOLD effect of tACS *vs*. sham, a measure of dose dependence that is orthogonal to the contrast of interest (in-phase *vs*. anti-phase). These expectations were preregistered at the Open Science Framework: (https://osf.io/j9s2z/).

**ROI masks**

The sensorimotor cortex (SMC) mask was created as a 10 mm spherical ROI centered at MNI coordinates [-36, -30, 72], based on model-based estimates of current density distribution under the SMC electrode location, along with the anatomical location used for neuronavigation. The dorsolateral prefrontal cortex (dlPFC) mask was derived from the right middle frontal gyrus mask in the probabilistic Harvard-Oxford Atlas (included in FSL). The bilateral amygdala mask was created using the right and left amygdala masks from the Harvard-Oxford Atlas, thresholded at 25%.

**fMRI analyses – preprocessing**

All image processing was performed using MELODIC 3.00, as implemented in FSL 6.0.0 (https://fsl.fmrib.ox.ac.uk; (Jenkinson et al., 2012)). Motion correction was applied using MCFLIRT (Jenkinson et al., 2002), while magnetic field distortions were corrected with TOPUP (Andersson et al., 2003). Functional images were rigid-body registered to the brain-extracted structural image using FLIRT (Jenkinson et al., 2002). Nonlinear registration to MNI 2 mm standard space was performed with FNIRT. Images were then spatially smoothed with a 5 mm Gaussian kernel, high-pass filtered at 100 s, and pre-whitened. Independent component analysis (ICA) was conducted with a maximum of 100 components (Beckmann and Smith, 2004), which were manually inspected to remove potential noise sources (Griffanti et al., 2017).

**fMRI analyses – GLM**

Emotional action control effects on whole-brain BOLD activation were estimated by contrasting incongruent trials (approach angry and avoid happy) with congruent trials (avoid angry and approach happy) across all stimulation conditions (in-phase, anti-phase, and sham).

tACS-dose effects on the whole-brain BOLD signal were assessed by comparing stimulation conditions (in-phase and anti-phase) to sham across both congruency conditions. Individual estimates of prefrontal tACS-dose were extracted from the 98% peak-activated voxel within the Harvard-Oxford middle frontal gyrus (dlPFC) mask. This tACS-dose metric (active tACS > sham tACS) is orthogonal to both the tACS-phase manipulation and the emotional action control contrast. Because concurrent fMRI-EEG studies have shown that low-frequency brain rhythms (e.g. theta) are associated with reduced BOLD signal (Scheeringa et al., 2009; Algermissen et al., 2022), in line with their predominantly inhibitory role (Yu et al., 2023; Leung and Yim, 2025), we consider a net reduction in prefrontal BOLD signal as a marker of stronger tACS-dose (see also Bramson et al., 2020a). Additionally, an exploratory whole-brain correlation analysis was conducted to examine the relationship between individual variation in STAI trait anxiety (*Z*-scored) and the tACS-dose contrast.

tACS-phase effects on congruency-related changes in dlPFC coupling were examined using generalized psychophysiological interaction (gPPI) analysis (O'Reilly et al., 2012). We created an interaction contrast between congruency (incongruent > congruent), tACS-phase (in-phase > anti-phase), and the mean dlPFC BOLD time series. The mean dlPFC signal for the seed regressor was extracted from a spherical ROI with a 5 mm radius, centered at each individual's peak tACS-dose location. tACS-phase effects on temporal BOLD signal coupling between dlPFC (seed) and SMC (target) were assessed using small volume correction. Cluster-based inference was performed using Gaussian Random Field Theory correction, as implemented in FSL's cluster tool (Smith and Nichols, 2009). A cluster-defining threshold of $|Z| = 2.3$ and a corrected cluster significance threshold of $p < 0.05$ were applied to control for multiple comparisons within the ROI.

First- and second-level GLM analyses were performed in FSL 6.0.5 using FEAT (Jenkinson et al., 2012). At the first level, the model included 12 task regressors: approach angry, approach happy, avoid angry, and avoid happy, modeled separately for each tACS condition (in-phase, anti-phase, and sham). Each regressor covered the time interval from stimulus presentation until joystick movement onset. The model also included nuisance regressors for estimated head motion (six

translation and rotation parameters), their temporal derivatives, and global signal time series from white matter and cerebrospinal fluid. First-level models from two separate stimulation sessions were combined using fixed effects analysis in FEAT (Jenkinson et al., 2012).

At the group level, effects were assessed using FLAME 1 with outlier de-weighting (Woolrich, 2008). Family-wise error correction was applied using cluster-based inference with a cluster-forming threshold of $|Z| > 2.3$, which provides a false error rate of approximately 5% when using FLAME 1 (Eklund et al., 2016).

316 **RESULTS**

317

318 **Behavioral cost of emotional action control**

319 Forty-nine participants, selected on high self-reported daily-life social anxiety (**Fig. 1A**), were
320 instructed to use a joystick to approach happy and avoid angry faces (affect-congruent condition)
321 or avoid happy and approach angry faces (affect-incongruent condition), **Fig. 1B**. The affect-
322 incongruent condition requires participants to override automatic emotional action tendencies to
323 avoid angry and approach happy faces (Roelofs et al., 2009a; Phaf et al., 2014). Expected
324 congruency effects were observed in the baseline sham-tACS condition, with higher error rates for
325 incongruent as compared to congruent responses ($b_{\text{congruency}}$ = 0.35, 95% *Confidence Interval* (*CI*)
326 [0.09, 0.62], $\chi^2_{(1)} = 7.06$, $p = 0.0079$) (Volman et al., 2011; Bramson et al., 2018, 2020a; Kaldewaij
327 et al., 2021), **Fig. 1C**. Specifically, the odds of participants making an incorrect response were 42%
328 higher in the incongruent as compared to congruent condition (*Odds Ratio* (*OR*) = 1.42, 95% *CI*
329 [1.10, 1.85]). This shows that exerting emotional action control is behaviorally costly.

330

331 **Socially anxious individuals recruit dlPFC for emotional action control**

332 The patterns of whole-brain neural activation largely aligned with previous findings using the same
333 task in non-anxious individuals, showing increased activation during incongruent *vs*. congruent
334 trials in bilateral precuneus [14, -70, 36], lingual gyrus [16, -74, -4], and right dorsal anterior
335 cingulate cortex [8, 32, 28], as well as decreased activity in bilateral medial [-8, 34, -14] and lateral
336 orbitofrontal cortex [-40, 28, -14; 24, 28, -14], temporal pole [-42, 16, -36], fusiform cortex [40, -
337 42, -18], amygdala [38, -4, -20], extending into hippocampus and parahippocampal gyrus (Volman
338 et al., 2011; Bramson et al., 2018, 2020a), **Table 1** and **Fig. 1D**. However, highly anxious
339 individuals exhibited more robust activation for incongruent trials in the dorsolateral prefrontal
340 cortex (dlPFC; Brodmann areas 9/46d) [30, 36, 38], rather than in the lateral frontal pole (FPl)
341 region previously found in non-anxious individuals (Bramson et al., 2020a; Kaldewaij et al., 2021;
342 Lapate et al., 2022). The differences in emotional action control circuits between high-anxious and
343 non-anxious individuals have been detailed in a separate paper (Bramson et al., 2023). These
344 findings indicate that high-anxious individuals likely implement control using dlPFC rather than
345 FPl as non-anxious individuals (Bramson et al., 2023).

346

**In-phase tACS strengthens dlPFC-SMC functional coupling**

We used simultaneous tACS and fMRI to verify neural consequences of the tACS-phase manipulation, **Fig. 2A**. In-phase *vs.* anti-phase tACS (**Fig. 2B**) selectively enhanced functional connectivity between dlPFC and SMC target regions under the congruency challenge, as quantified using generalized psychophysiological interaction (gPPI) analysis (SMC cluster: $Z_{max} = 3.2$, $p_{fwe} = 0.0184$, MNI[-36, -26, 68]), **Fig. 2C**. This finding underscores the specificity of the in-phase tACS manipulation in strengthening inter-regional dlPFC-SMC coupling.

**Facilitation of emotional action control scales with dlPFC target engagement**

Concurrent tACS-fMRI was used to study the underlying mechanisms of dual-site tACS effects, as well as to explain inter-individual variance in facilitation of behavioral performance depending on prefrontal stimulation reactivity. Following our pre-registered analysis pipeline (https://osf.io/j9s2z), we evaluated the cerebral effects of prefrontal tACS by examining BOLD activity in the region involved in implementing emotional action control in these high-anxious participants. Given that high-anxious individuals recruit dlPFC to solve emotional action control (Bramson et al., 2023), and that the dual-site tACS montage of this study evokes electrical fields covering dlPFC, we choose dlPFC BOLD activity as a metric of tACS dose-response. As in (Bramson et al., 2020a), the tACS-dose metric is obtained from a BOLD contrast (active tACS > sham tACS) that is orthogonal to both the tACS-phase manipulation and the emotional action control contrast. and we consider a net reduction in prefrontal BOLD signal as a marker of stronger tACS-dose (Scheeringa et al., 2009; Bramson et al., 2020a). Critically, we observe tACS-dose and tACS-phase specific enhancement of emotional action control ($b_{dlPFC\text{-}dose} = -0.34$, 95% CI [-0.66, -0.02], $\chi^2_{(1)} = 4.43$, $p = 0.0353$), **Fig. 3A**. Participants with a more robust inhibitory response to prefrontal tACS exhibited greater improvement in emotional action control when receiving in-phase as opposed to anti-phase tACS. Planned post-hoc analyses on congruency-related error rates confirm significant dose-dependent effects for the in-phase (Spearman's $\rho_{(47)} = 0.37$, $p = .0092$) but not for the anti-phase condition (Spearman's $\rho_{(47)} = -0.09$, $p = .5194$). The direction and magnitude of the dual-site in-phase tACS intervention effects align with our previous report (Bramson et al., 2020a), and were specifically linked to tACS-dose measured over dlPFC. Namely, when extracting tACS-dose from FPl, a region previously reported to be decoupled from emotional action control in high-anxious individuals (Bramson et al., 2023), no significant tACS-induced changes in emotional action control were observed ($b_{FPl\text{-}dose} = -0.12$, 95% CI [-0.46, 0.22], $\chi^2_{(1)} = 0.49$, $p = 0.4844$). Further exploration of brain-symptoms correlations revealed a positive association between higher trait anxiety levels and stronger tACS-dose in dlPFC, **Fig. 3B**. In summary, the

findings demonstrate that dual-site tACS can effectively enhance emotional action control in high-anxious individuals by targeting phase-amplitude coupling between dlPFC and SMC.

**In-phase tACS improves valence-based action selection**

We also examined tACS-phase effects independent of tACS-dose. In-phase tACS, but not anti-phase tACS, results in a general behavioral performance enhancement compared to sham ($b_{\text{tACS-phase}}$ = -0.16, *SE* = 0.08, $p$ = 0.0403), **Fig. 3C**. Specifically, in-phase tACS reduces the odds of participants making an incorrect response by 22% across both congruency conditions compared to sham ($b_{\text{in-phase}}$ = -0.25, 95% *CI* = [-0.39, -0.11], $p$ = 0.0004; *OR* = 0.78, 95% *CI* = [0.67, 0.89]). In contrast, anti-phase tACS had no significant effect on behavioral accuracy ($b_{\text{anti-phase}}$ = -0.10, 95% *CI* = [-0.25, 0.06], $p$ = 0.2225). Consistent with our previous work (Bramson et al., 2020a), when individual differences in neural responsiveness to tACS were not controlled for, tACS-phase did not show a congruency-specific effect on performance ($\chi^2_{(2)}$ = 0.85, $p$ = 0.6548).

Next, we explored the neural mechanisms underlying the general improvement in valence-based action selection during in-phase tACS. Given prior evidence that emotion control involves amygdala dampening (Volman et al., 2011, 2013, 2016) and that suppression of task-irrelevant valence signals reduces amygdala engagement (Anticevic et al., 2010; Kanske et al., 2011; Cohen et al., 2016) we focused on amygdala activation (bilateral). We find a significant effect of tACS-phase on congruency-dependent amygdala modulation ($b_{\text{congruency:tACS-phase}}$ = 0.05, 95% CI = [0.00, 0.09], $F_{(1, 96)}$ = 4.62, $p$ = 0.0341, $\eta_p^2$ = 0.05), **Fig. 3D**. Specifically, in-phase tACS resulted in stronger congruency-related modulation of amygdala activation ($b_{\text{congruency}}$ = 0.06, $t_{(95)}$ = 3.47, $p$ = 0.0008) compared to anti-phase tACS, which showed no significant effect ($b_{\text{congruency}}$ = 0.01, $t_{(95)}$ = 0.62, $p$ = 0.5355). Together, these findings suggest that in-phase tACS facilitation of dlPFC-SMC coupling enhances valence signal processing based on the affect-congruency of action goals, in a dose-response manner, and supports amygdala contribution to affect-congruent responses.

408 **DISCUSSION** (1239/1500)

409

410 This study demonstrates that in-phase dual-site tACS, targeted at facilitating endogenous theta-
411 gamma phase-amplitude coupling between lPFC and SMC, enhances control over emotional action
412 tendencies in highly socially anxious individuals. The main finding is that dual-site tACS effects,
413 previously reported to improve control over automatic approach-avoidance tendencies in non-
414 anxious participants (Bramson et al., 2020a), generalize to a clinically relevant population with
415 altered control over daily-life social-emotional behavior (LSAS ≥ 30) (Mennin et al., 2002; Roelofs
416 et al., 2009b; van Peer et al., 2009). Furthermore, this study shows that the dual-site tACS
417 intervention in high-anxious males and females evokes effects in a different prefrontal territory
418 (dlPFC) than in non-anxious males (FPl) (Bramson et al., 2020a). This observation fits the recently
419 reported shift in the prefrontal circuit implementing emotional action control from FPl (non-anxious
420 participants) to dlPFC (high-anxious participants) (Bramson et al., 2023). The current study
421 demonstrates the possibility of improving emotional action control using dual-site tACS in high-
422 anxious individuals via the facilitation of endogenous long-range phase-amplitude coupling. This
423 finding extends our mechanistic understanding of approach-avoidance control in social anxiety and
424 introduces rhythmic synchronization between dlPFC and SMC as a novel therapeutic tool.

425

426 **dlPFC-SMC phase-amplitude coupling supports emotional action control in social anxiety**

427 This dual-site tACS intervention builds on prior studies that have demonstrated the significance of
428 endogenous lPFC-SMC theta-gamma coupling in controlling automatic emotional action
429 tendencies and in facilitating the implementation of alternative goal-directed actions (Bramson et
430 al., 2018, 2020a). In this study, in-phase dual-site tACS could enhance interregional
431 synchronization of neuronal excitability periods, biasing action selection in SMC according to
432 valence-incongruent action goals in dlPFC (Voytek et al., 2015; Bramson et al., 2018; Weber et al.,
433 2024). In one important detail, this putative mechanism differs from what has been observed in
434 healthy individuals, where prefrontal control emerged from FPl (Bramson et al., 2020a) rather than
435 dlPFC (this study). This difference is important for understanding the scope and the mechanism of
436 the dual-site tACS intervention in social anxiety. Namely, FPl is a region that can flexibly integrate
437 valence signals with approach-avoid action selection, allowing FPl to orchestrate goal-directed
438 control over automatic emotional action tendencies (Bramson et al., 2020b; Lapate et al., 2022).
439 However, FPl is overexcitable in high-anxious individuals (Bramson et al., 2023), and the evidence
440 suggests dlPFC compensates for FPl when control over emotional actions is required (Bramson et
441 al., 2023). In contrast with integrated valence-action goal representations observed in FPl, action

goal representations in dlPFC are not modulated by valence (Lapate et al., 2022), consistent with relatively sparse mono-synaptic connections from amygdala to dlPFC (Petrides and Pandya, 1999; Folloni et al., 2019). In fact, dlPFC engagement could dampen amygdala processing via strong indirect projections to the ventromedial subgenual cingulate area 25 (Joyce et al., 2020, 2023), thereby providing a candidate mechanism for gating the contribution of emotional afferences to cognitive control (Berboth and Morawetz, 2021). Thus, the dlPFC can implement rule-based actions with minimal interference from emotional valence signals even in high anxiety, when emotional signals would saturate an already overexcitable FPl (Bramson et al., 2023). However, this may come at a cost: dlPFC-based emotional action control might be limited when emotional challenges co-occur with demands for cognitive control, e.g. during real-life situations. Accordingly, high-anxious individuals show reduced dlPFC efficiency during cognitive control compared to non-anxious individuals (Eysenck et al., 2022). It remains to be seen whether dual-site tACS in socially-anxious individuals can enhance dlPFC coordination with SMC and remain behaviorally effective even in the presence of multiple cognitive control demands.

**tACS BOLD dose-response in dlPFC scales with trait anxiety**

The current study shows that the application of in-phase dual-site tACS results in behavioral effects proportional to BOLD signal evoked over dlPFC across tACS conditions, i.e., a dose-response effect. We also observe that individuals with higher trait anxiety exhibit more robust dlPFC responses to the tACS intervention. This finding corresponds to the observation that trait anxiety is associated with an anatomical shift of prefrontal emotional action control, from FPl to dlPFC (Bramson et al., 2023). The link between tACS response and trait anxiety signals that sub-optimal endogenous synchronization could underlie reduced emotion control performance in anxiety. Namely, the most robust effects of tACS are expected when weak endogenous oscillations can be facilitated (Krause et al., 2022), and in-phase dual-site tACS is expected to improve long-range communication by reducing noise within hypo-synchronized circuits (Wischnewski et al., 2023). Specifically, we suggest that trait anxiety might index individual levels of neural noise within the dlPFC-SMC circuit during emotional action control, a prediction that could be tested by measuring electrophysiological activity during emotional action control in high-anxious individuals (Bramson et al., 2018). This knowledge would be instrumental in facilitating the translation of dual-site tACS to clinical protocols, as it would enable using trait anxiety rather than concurrent tACS-fMRI to estimate individual dose-responses.

**Interpretational issues and future directions**

It could be argued that the current findings are limited by the lack of electrophysiological observations of the consequences of tACS. In fact, the manipulation of dual-site tACS phase angle (in-phase *versus* anti-phase) enables us to relate the tACS effects to phase-specific changes in long-range phase-amplitude coupling, and exclude general changes in lPFC or SMC excitability. The phase manipulation provides the additional benefit of fully matching peripheral effects between in-phase and anti-phase stimulation, thereby ruling out alternative explanations related to transcutaneous entrainment or retinal stimulation (Schutter, 2016; Asamoah et al., 2019).

In this study, phase-specific dual-site tACS improvements in emotional action control are dose-related, an indication of high inter-individual variation in the effects of dual-site tACS on emotional action control. This variation makes the tACS effects physiologically plausible, since tACS effects depends on the electric field induced in the brain (Krause et al., 2019; Johnson et al., 2020) and on the interaction with ongoing endogenous oscillations (Krause et al., 2022). Future studies could use individualized current flow models to optimize stimulation protocols and enhance targeting accuracy to achieve more consistent tACS effects (Grover et al., 2023). However, these models do not capture state-dependent effects in the neural response to stimulation (Bradley et al., 2022), which could be particularly relevant for translational efforts in which the neural mechanisms underlying the disorder are not fully understood. Inter-individual variation in tACS efficacy can be exploited to identify factors that could maximize intervention response, in particular when used to enhance the effectiveness of existing treatments. This can include improving the ability to control emotional behavior during exposure therapy to confront threatening situations and temporarily interrupt the cycle of persistent avoidance.

## CONCLUSION

Building non-invasive neuromodulation interventions that facilitate cognitive function presents a major neuroscientific challenge due to the need to identify and enhance the underlying endogenous neural dynamics. Translating mechanistically informed neuromodulation interventions from healthy individuals to clinical populations poses a further challenge due to an incomplete understanding of the neural mechanisms underlying psychiatric disorders. Here, we successfully translate a mechanistically informed dual-site tACS intervention (Bramson et al., 2018, 2020a) to a clinically relevant high-anxiety population that shows impairments in daily-life social-emotional behavior. The findings highlight the advantage of combining cognitive neuromodulation interventions with neuroimaging during the early stages of clinical translation. The advantage of

this multi-modal approach is that it offers a better understanding of the intervention mechanism, leading to a more precise characterization of inter-individual variation in intervention response. The results provide insights into the role of phase-amplitude coupling between lPFC and SMC in emotion control over social approach-avoidance behavior and contribute to developing targeted clinical interventions for anxiety.

515 **REFERENCES**


516 Algermissen J, Swart JC, Scheeringa R, Cools R, den Ouden HEM (2022) Striatal BOLD and midfrontal theta power
517 express motivation for action. Cereb Cortex 32:2924–2942.

518 Andersson JLR, Skare S, Ashburner J (2003) How to correct susceptibility distortions in spin-echo echo-planar
519 images: application to diffusion tensor imaging. NeuroImage 20:870–888.

520 Anticevic A, Barch DM, Repovs G (2010) Resisting emotional interference: Brain regions facilitating working
521 memory performance during negative distraction. Cognitive, Affective, & Behavioral Neuroscience 10:159–
522 173.

523 Asamoah B, Khatoun A, Mc Laughlin M (2019) tACS motor system effects can be caused by transcutaneous
524 stimulation of peripheral nerves. Nat Commun 10:266.

525 Bates D, Mächler M, Bolker B, Walker S (2015) Fitting Linear Mixed-Effects Models Using lme4. Journal of
526 Statistical Software 67:1–48.

527 Beckmann CF, Smith SM (2004) Probabilistic independent component analysis for functional magnetic resonance
528 imaging. IEEE Transactions on Medical Imaging 23:137–152.

529 Berboth S, Morawetz C (2021) Amygdala-prefrontal connectivity during emotion regulation: A meta-analysis of
530 psychophysiological interactions. Neuropsychologia 153:107767.

531 Bradley C, Nydam AS, Dux PE, Mattingley JB (2022) State-dependent effects of neural stimulation on brain function
532 and cognition. Nat Rev Neurosci 23:459–475.

533 Bramson B, den Ouden HE, Toni I, Roelofs K (2020a) Improving emotional-action control by targeting long-range
534 phase-amplitude neuronal coupling Shackman A, Ivry RB, eds. eLife 9:e59600.

535 Bramson B, Folloni D, Verhagen L, Hartogsveld B, Mars RB, Toni I, Roelofs K (2020b) Human Lateral Frontal Pole
536 Contributes to Control over Emotional Approach–Avoidance Actions. J Neurosci 40:2925–2934.

537 Bramson B, Jensen O, Toni I, Roelofs K (2018) Cortical Oscillatory Mechanisms Supporting the Control of Human
538 Social–Emotional Actions. J Neurosci 38:5739–5749.

539 Bramson B, Meijer S, van Nuland A, Toni I, Roelofs K (2023) Anxious individuals shift emotion control from lateral
540 frontal pole to dorsolateral prefrontal cortex. Nat Commun 14:4880.

541 Cohen N, Margulies DS, Ashkenazi S, Schaefer A, Taubert M, Henik A, Villringer A, Okon-Singer H (2016) Using
542 executive control training to suppress amygdala reactivity to aversive information. NeuroImage 125:1022–
543 1031.

544 Craske MG, Stein MB (2016) Anxiety. The Lancet 388:3048–3059.

545 Eklund A, Nichols TE, Knutsson H (2016) Cluster failure: Why fMRI inferences for spatial extent have inflated
546 false-positive rates. Proceedings of the National Academy of Sciences 113:7900–7905.

547 Eysenck MW, Moser JS, Derakshan N, Hepsomali P, Allen P (2022) A neurocognitive account of attentional control
548 theory: how does trait anxiety affect the brain's attentional networks? Cognition and Emotion 0:1–18.

549 Faul F, Erdfelder E, Lang A-G, Buchner A (2007) G*Power 3: A flexible statistical power analysis program for the
550 social, behavioral, and biomedical sciences. Behavior Research Methods 39:175–191.

551 Folloni D, Sallet J, Khrapitchev AA, Sibson N, Verhagen L, Mars RB (2019) Dichotomous organization of
552 amygdala/temporal-prefrontal bundles in both humans and monkeys Heilbronner S, Gold JI, Thiebaut de
553 Schotten M, eds. eLife 8:e47175.

554 Griffanti L, Douaud G, Bijsterbosch J, Evangelisti S, Alfaro-Almagro F, Glasser MF, Duff EP, Fitzgibbon S,
555 Westphal R, Carone D, Beckmann CF, Smith SM (2017) Hand classification of fMRI ICA noise
556 components. NeuroImage 154:188–205.

557 Grover S, Fayzullina R, Bullard BM, Levina V, Reinhart RMG (2023) A meta-analysis suggests that tACS improves
558 cognition in healthy, aging, and psychiatric populations. Science Translational Medicine 15:eabo2044.

559 Grover S, Wen W, Viswanathan V, Gill CT, Reinhart RMG (2022) Long-lasting, dissociable improvements in
560 working memory and long-term memory in older adults with repetitive neuromodulation. Nat Neurosci
561 25:1237–1246.

562 Heuer K, Rinck M, Becker ES (2007) Avoidance of emotional facial expressions in social anxiety: The Approach–
563 Avoidance Task. Behaviour Research and Therapy 45:2990–3001.

564 Jenkinson M, Bannister P, Brady M, Smith S (2002) Improved Optimization for the Robust and Accurate Linear
565 Registration and Motion Correction of Brain Images. NeuroImage 17:825–841.

566 Jenkinson M, Beckmann CF, Behrens TEJ, Woolrich MW, Smith SM (2012) FSL. NeuroImage 62:782–790.

567 Johnson L, Alekseichuk I, Krieg J, Doyle A, Yu Y, Vitek J, Johnson M, Opitz A (2020) Dose-dependent effects of
568 transcranial alternating current stimulation on spike timing in awake nonhuman primates. Science Advances
569 6:eaaz2747.

570 Joyce MKP, García-Cabezas MÁ, John YJ, Barbas H (2020) Serial Prefrontal Pathways Are Positioned to Balance
571 Cognition and Emotion in Primates. J Neurosci 40:8306–8328.

572 Joyce MKP, Wang J, Barbas H (2023) Subgenual and Hippocampal Pathways in Amygdala Are Set to Balance
573 Affect and Context Processing. J Neurosci 43:3061–3080.

574 Kaldewaij R, Koch SBJ, Hashemi MM, Zhang W, Klumpers F, Roelofs K (2021) Anterior prefrontal brain activity
575 during emotion control predicts resilience to post-traumatic stress symptoms. Nat Hum Behav 5:1055–1064.

576 Kanske P, Heissler J, Schönfelder S, Bongers A, Wessa M (2011) How to Regulate Emotion? Neural Networks for
577 Reappraisal and Distraction. Cerebral Cortex 21:1379–1388.

578 Koch SBJ, Mars RB, Toni I, Roelofs K (2018) Emotional control, reappraised. Neuroscience & Biobehavioral
579 Reviews 95:528–534.

580 Krause MR, Vieira PG, Csorba BA, Pilly PK, Pack CC (2019) Transcranial alternating current stimulation entrains
581 single-neuron activity in the primate brain. Proceedings of the National Academy of Sciences 116:5747–
582 5755.

583 Krause MR, Vieira PG, Thivierge J-P, Pack CC (2022) Brain stimulation competes with ongoing oscillations for
584 control of spike timing in the primate brain. PLOS Biology 20:e3001650.

585 Lapate RC, Ballard IC, Heckner MK, D'Esposito M (2022) Emotional Context Sculpts Action Goal Representations
586 in the Lateral Frontal Pole. J Neurosci 42:1529–1541.

587 Leung LS, Yim CYC (2025) Inhibitory Postsynaptic Potentials Participate in Intracellular and Extracellular Theta
588 Rhythms in the Hippocampus: A Personal Narrative. Hippocampus 35:e23660.

589 Lovibond PF, Mitchell CJ, Minard E, Brady A, Menzies RG (2009) Safety behaviours preserve threat beliefs:
590 Protection from extinction of human fear conditioning by an avoidance response. Behaviour Research and
591 Therapy 47:716–720.

592 Mennin DS, Fresco DM, Heimberg RG, Schneier FR, Davies SO, Liebowitz MR (2002) Screening for social anxiety
593 disorder in the clinical setting: using the Liebowitz Social Anxiety Scale. J Anxiety Disord 16:661–673.

594 Neubert F-X, Mars RB, Thomas AG, Sallet J, Rushworth MFS (2014) Comparison of Human Ventral Frontal Cortex
595 Areas for Cognitive Control and Language with Areas in Monkey Frontal Cortex. Neuron 81:700–713.

596 O'Reilly JX, Woolrich MW, Behrens TEJ, Smith SM, Johansen-Berg H (2012) Tools of the trade:
597 psychophysiological interactions and functional connectivity. Soc Cogn Affect Neurosci 7:604–609.

598 Petrides M, Pandya DN (1999) Dorsolateral prefrontal cortex: comparative cytoarchitectonic analysis in the human
599 and the macaque brain and corticocortical connection patterns. European Journal of Neuroscience 11:1011–
600 1036.

601 Phaf RH, Mohr SE, Rotteveel M, Wicherts JM (2014) Approach, avoidance, and affect: a meta-analysis of approach-
602 avoidance tendencies in manual reaction time tasks. Frontiers in Psychology 5 Available at:
603 https://www.frontiersin.org/articles/10.3389/fpsyg.2014.00378 [Accessed April 17, 2023].

604 Pittig A, Alpers GW, Niles AN, Craske MG (2015) Avoidant decision-making in social anxiety disorder: A
605 laboratory task linked to in vivo anxiety and treatment outcome. Behaviour Research and Therapy 73:96–
606 103.

607 Polanía R, Nitsche MA, Korman C, Batsikadze G, Paulus W (2012) The Importance of Timing in Segregated Theta
608 Phase-Coupling for Cognitive Performance. Current Biology 22:1314–1318.

609 Preisig BC, Riecke L, Sjerps MJ, Kösem A, Kop BR, Bramson B, Hagoort P, Hervais-Adelman A (2021) Selective
610 modulation of interhemispheric connectivity by transcranial alternating current stimulation influences
611 binaural integration. Proceedings of the National Academy of Sciences 118:e2015488118.

612 Rattel JA, Miedl SF, Blechert J, Wilhelm FH (2017) Higher threat avoidance costs reduce avoidance behaviour which
613 in turn promotes fear extinction in humans. Behaviour Research and Therapy 96:37–46.

614 Reinhart RMG, Nguyen JA (2019) Working memory revived in older adults by synchronizing rhythmic brain
615 circuits. Nat Neurosci 22:820–827.

616 Roelofs K, Minelli A, Mars RB, van Peer J, Toni I (2009a) On the neural control of social emotional behavior. Social
617 Cognitive and Affective Neuroscience 4:50–58.

618 Roelofs K, van Peer J, Berretty E, Jong P de, Spinhoven P, Elzinga BM (2009b) Hypothalamus–Pituitary–Adrenal
619 Axis Hyperresponsiveness Is Associated with Increased Social Avoidance Behavior in Social Phobia.
620 Biological Psychiatry 65:336–343.

621 Saturnino GB, Madsen KH, Siebner HR, Thielscher A (2017) How to target inter-regional phase synchronization
622 with dual-site Transcranial Alternating Current Stimulation. NeuroImage 163:68–80.

623 Scheeringa R, Fries P, Petersson K-M, Oostenveld R, Grothe I, Norris DG, Hagoort P, Bastiaansen MCM (2011)
624 Neuronal Dynamics Underlying High- and Low-Frequency EEG Oscillations Contribute Independently to
625 the Human BOLD Signal. Neuron 69:572–583.

626 Scheeringa R, Petersson KM, Oostenveld R, Norris DG, Hagoort P, Bastiaansen MCM (2009) Trial-by-trial coupling
627 between EEG and BOLD identifies networks related to alpha and theta EEG power increases during
628 working memory maintenance. NeuroImage 44:1224–1238.

629 Schutter DJLG (2016) Cutaneous retinal activation and neural entrainment in transcranial alternating current
630 stimulation: A systematic review. NeuroImage 140:83–88.

631 Smith SM, Nichols TE (2009) Threshold-free cluster enhancement: Addressing problems of smoothing, threshold
632 dependence and localisation in cluster inference. NeuroImage 44:83–98.

633 Thielscher A, Antunes A, Saturnino GB (2015) Field modeling for transcranial magnetic stimulation: A useful tool to
634 understand the physiological effects of TMS? In: 2015 37th Annual International Conference of the IEEE
635 Engineering in Medicine and Biology Society (EMBC), pp 222–225.

636 van Peer JM, Spinhoven P, Dijk JG van, Roelofs K (2009) Cortisol-induced enhancement of emotional face
637 processing in social phobia depends on symptom severity and motivational context. Biological Psychology
638 81:123–130.

Violante IR, Li LM, Carmichael DW, Lorenz R, Leech R, Hampshire A, Rothwell JC, Sharp DJ (2017) Externally induced frontoparietal synchronization modulates network dynamics and enhances working memory performance Hamilton R, ed. eLife 6:e22001.

Volman I, Borries AKL von, Bulten BH, Verkes RJ, Toni I, Roelofs K (2016) Testosterone Modulates Altered Prefrontal Control of Emotional Actions in Psychopathic Offenders. eNeuro 3 Available at: https://www.eneuro.org/content/3/1/ENEURO.0107-15.2016 [Accessed March 19, 2025].

Volman I, Roelofs K, Koch S, Verhagen L, Toni I (2011) Anterior Prefrontal Cortex Inhibition Impairs Control over Social Emotional Actions. Current Biology 21:1766–1770.

Volman I, Verhagen L, Ouden HEM den, Fernández G, Rijpkema M, Franke B, Toni I, Roelofs K (2013) Reduced Serotonin Transporter Availability Decreases Prefrontal Control of the Amygdala. J Neurosci 33:8974–8979.

Voytek B, Kayser AS, Badre D, Fegen D, Chang EF, Crone NE, Parvizi J, Knight RT, D'Esposito M (2015) Oscillatory dynamics coordinating human frontal networks in support of goal maintenance. Nat Neurosci 18:1318–1324.

Weber J, Solbakk A-K, Blenkmann AO, Llorens A, Funderud I, Leske S, Larsson PG, Ivanovic J, Knight RT, Endestad T, Helfrich RF (2024) Ramping dynamics and theta oscillations reflect dissociable signatures during rule-guided human behavior. Nat Commun 15:637.

Wischnewski M, Alekseichuk I, Opitz A (2023) Neurocognitive, physiological, and biophysical effects of transcranial alternating current stimulation. Trends in Cognitive Sciences 27:189–205.

Woolrich M (2008) Robust group analysis using outlier inference. NeuroImage 41:286–301.

Yu S, Stock A-K, Münchau A, Frings C, Beste C (2023) Neurophysiological principles of inhibitory control processes during cognitive flexibility. Cereb Cortex 33:6656–6666.

662 **FIGURE LEGENDS**

663

664 ***Figure 1. Behavioral and BOLD fMRI effects related to control over emotional action***
665 ***tendencies. (A) Sample distribution of self-reported Liebowitz Social Anxiety Scale (LSAS)***
666 ***scores.*** *The black dashed line marks an LSAS score of 30, used to select socially anxious*
667 *participants. This cut-off balances specificity and sensitivity in detecting heightened social anxiety*
668 (Mennin et al., 2002). ***(B) Conceptual visualization of the approach-avoidance task performed***
669 ***during concurrent dual-site tACS and fMRI****. In affect-congruent conditions, participants were*
670 *instructed to pull the joystick towards them in response to a happy face and push it away from them*
671 *in response to an angry face. In contrast, the affect-incongruent condition requires participants to*
672 *override automatic emotional action tendencies to avoid angry and approach happy faces.*
673 *Therefore, in this condition, participants were instructed to pull the joystick towards them in*
674 *response to an angry face and push it away in response to a happy face.* ***(C) Behavioral***
675 ***congruency-effects in the baseline sham stimulation condition of the task.*** *Participants made*
676 *more errors when overriding their automatic emotional action tendencies in the affect-incongruent*
677 *condition (orange circles) as compared to making affect-congruent responses (blue circles). Black-*
678 *filled diamonds represent mean values, and standard errors of the mean are shown with black lines.*
679 ***(D) Task-fMRI congruency-related effects across tACS stimulation conditions*** *(incongruent >*
680 *congruent; cluster-level inferences corrected for multiple comparisons). Stronger BOLD signals*
681 *were observed in prefrontal- and parietal areas when automatic emotional action tendencies*
682 *needed to be overridden, while amygdala-hippocampal and medial-orbitofrontal areas showed*
683 *weaker BOLD signals.*

684

685 ***Figure 2. Dual-site phase-amplitude coupled tACS modulates endogenous inter-regional***
686 ***coupling between stimulation targets. (A) Modeled current density distribution at cortical targets.***
687 *Two sets of concentric ring electrodes were placed over the right lPFC and left SMC. The current*
688 *density model shows the spatial distribution of the electric field magnitude evoked by the high-*
689 *definition montage at both cortical targets.* ***(B) Dual-site phase-locked tACS manipulations.*** *The*
690 *stimulation conditions underwent a pseudo-random alternation throughout the experiment between*
691 *active in-phase tACS (green), active control anti-phase tACS (brown), and baseline sham (black).*
692 *Specifically, 75 Hz stimulation was administered over the SMC and its amplitude modulated by the*
693 *phase of a 6 Hz stimulation over the lPFC. Modulation was either in-phase or anti-phase with the*
694 *peaks of the 6 Hz lPFC stimulation. While both in-phase and anti-phase tACS may influence local*
695 *target excitability, in-phase tACS is specifically designed to enhance endogenous phase-amplitude*

*coupling between the dlPFC and SMC, a mechanism associated with successful emotional action control* (Bramson et al., 2018, 2020a). *The baseline sham condition involved a brief 10-second initial stimulation that was discontinued before the start of the first trial.* ***(C) tACS-phase effect on congruency-related dlPFC-SMC coupling.*** *In-phase vs. anti-phase tACS selectively increased congruency-related functional coupling between dlPFC (seed) and SMC (target) stimulation areas (in-phase > anti-phase * incongruent > congruent), confirming the effectiveness of the tACS-phase manipulation in modulating inter-regional functional connectivity supporting emotional action control.*

***Figure 3. Phase- and dose-specific effects of dual-site tACS on emotional action control in social anxiety. (A) In-phase tACS facilitation of emotional action control is dose-dependent.*** *Participants who exhibited stronger inhibitory theta-band stimulation responses in dlPFC, as evidenced by a decrease in BOLD signal* (Scheeringa et al., 2011; Bramson et al., 2020a), *demonstrated improved control over emotional actions (i.e., a reduced congruency effect) during in-phase tACS (green) compared to anti-phase tACS (brown). Black lines represent the fitted linear trend, with the shaded area indicating the associated 95% confidence interval.* ***(B) tACS-dose scales with trait anxiety.*** *Concurrent tACS-fMRI BOLD signal changes across the in-phase and anti-phase tACS conditions (tACS-dose: tACS > sham) correlated with trait anxiety, indicating a stronger inhibitory dlPFC dose-response in individuals with higher trait anxiety levels. To illustrate this relationship, we included a scatterplot depicting the association between trait anxiety scores and tACS-dose values extracted from the maximum Z-value location within dlPFC.* ***(C) In-phase tACS improves general behavioral performance independent of tACS-dose.*** *In-phase (green panel) vs. anti-phase tACS (brown panel) selectively enhanced response accuracy across congruent (blue) and incongruent (orange) conditions compared to sham. Bar plots represent mean and standard error of the mean for each condition, with individual participant means indicated by grey dots.* ***(D) In-phase tACS of dlPFC-SMC coupling modulates amygdala contribution to valence-based action selection.*** *Left: In the in-phase tACS condition, the right amygdala exhibited negative congruency-related BOLD signal (incongruent > congruent; cluster-level inferences corrected for multiple comparisons). White outlines indicate the anatomical bilateral amygdala mask used for extracting beta parameter estimates. Right: In-phase tACS (green panel) increased congruency-related amygdala modulation compared to anti-phase tACS (brown panel).*

## TABLE LEGEND

***Table 1.*** *Group-level effects in the whole-brain BOLD-GLM analysis were assessed using FSL's FLAME 1 mixed-effects model with automatic outlier de-weighting. Cluster-level inferences were family-wise error-corrected, applying a cluster-forming threshold of* $|Z| > 2.3$ *and* $p < 0.05$.

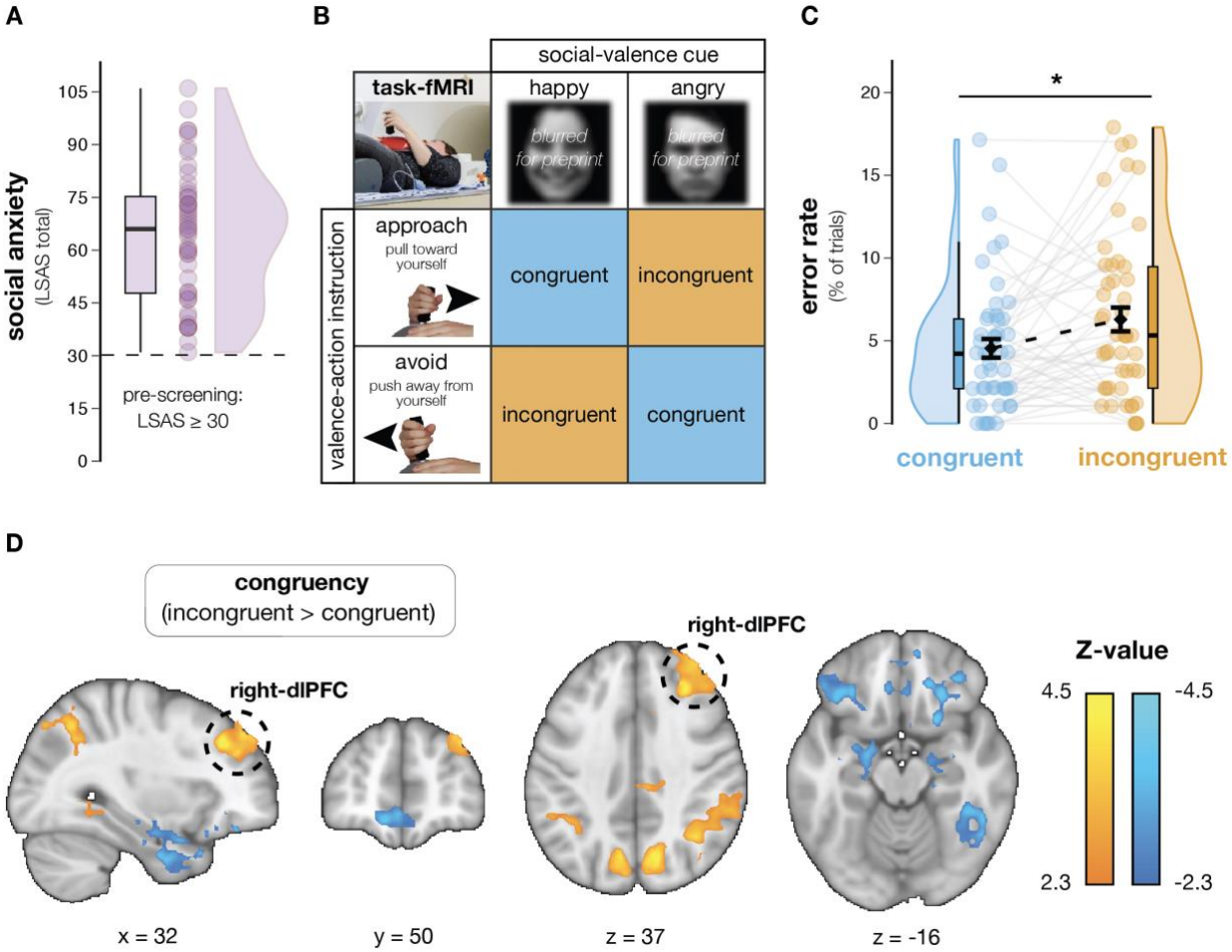
A
social anxiety
(LSAS total)
105
90
75
60
45
30
15
0
pre-screening:
LSAS ≥ 30
B
social-valence cue
task-fMRI
happy
angry
blurred for preprint
blurred for preprint
valence-action instruction
approach
pull toward yourself
congruent
incongruent
avoid
push away from yourself
incongruent
congruent
C
*
error rate
(% of trials)
20
15
10
5
0
congruent
incongruent
D
congruency
(incongruent > congruent)
right-dlPFC
right-dlPFC
Z-value
4.5
-4.5
2.3
-2.3
x = 32
y = 50
z = 37
z = -16

734

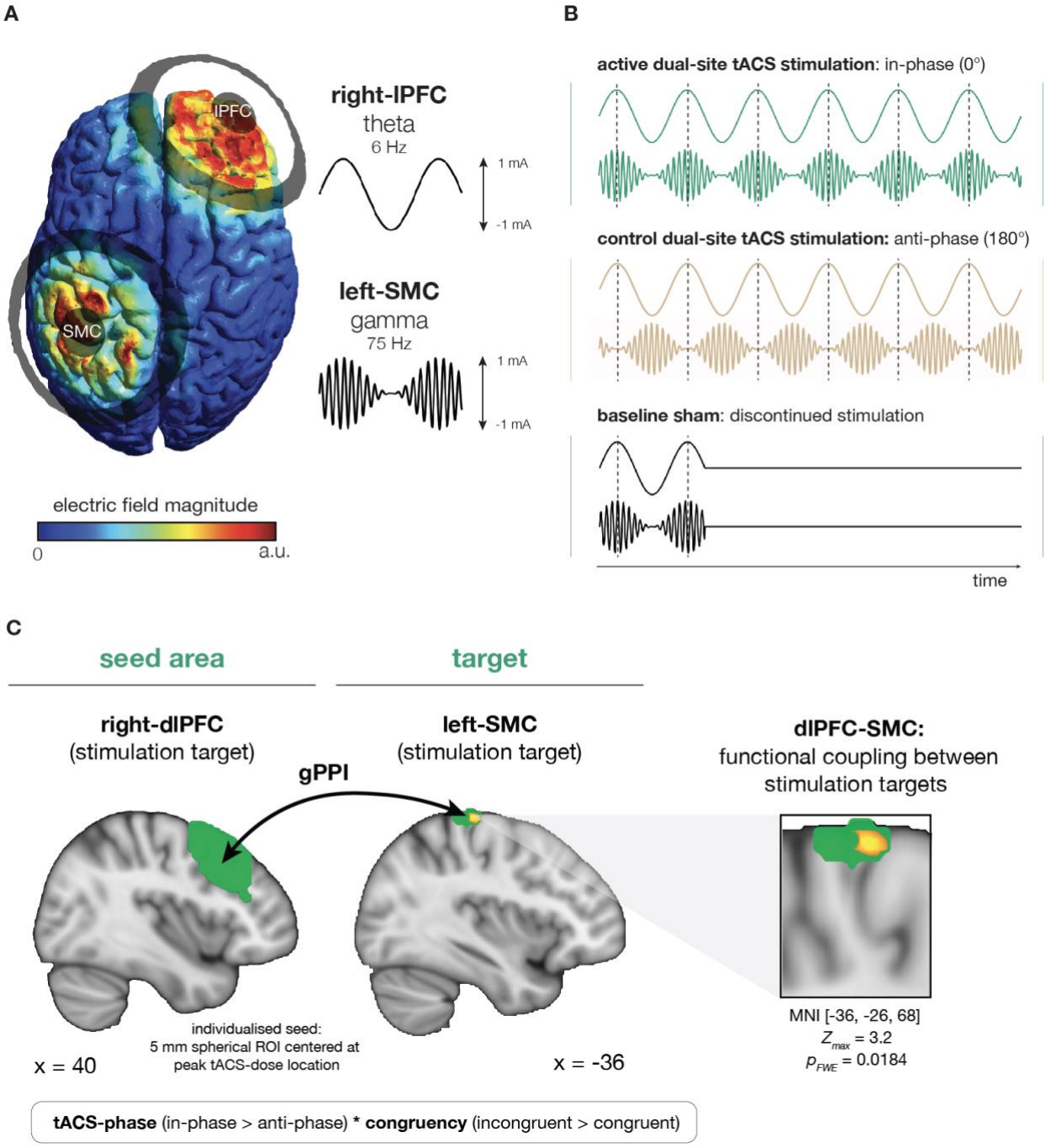
A
IPFC
SMC
right-lPFC
theta
6 Hz
1 mA
-1 mA
left-SMC
gamma
75 Hz
1 mA
-1 mA
electric field magnitude
0
a.u.
B
active dual-site tACS stimulation: in-phase (0°)
control dual-site tACS stimulation: anti-phase (180°)
baseline sham: discontinued stimulation
time
C
seed area
target
right-dlPFC
(stimulation target)
left-SMC
(stimulation target)
gPPI
dlPFC-SMC:
functional coupling between
stimulation targets
individualised seed:
5 mm spherical ROI centered at
peak tACS-dose location
x = 40
x = -36
MNI [-36, -26, 68]
$Z_{max}$ = 3.2
$p_{FWE}$ = 0.0184
tACS-phase (in-phase > anti-phase) * congruency (incongruent > congruent)

735

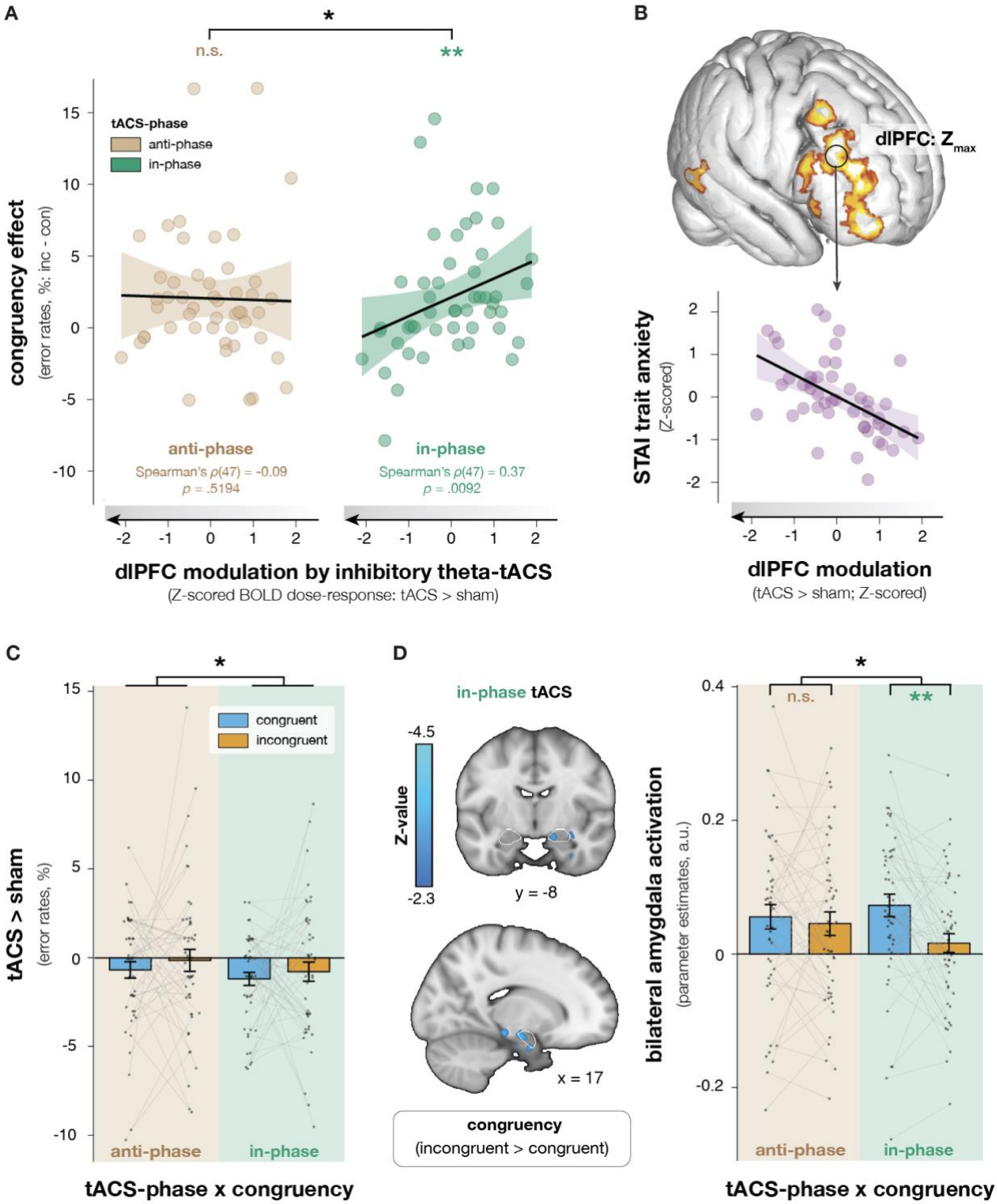
A
*
n.s.
**
tACS-phase
anti-phase
in-phase
congruency effect
(error rates, %: inc - con)
anti-phase
Spearman's ρ(47) = -0.09
p = .5194
in-phase
Spearman's ρ(47) = 0.37
p = .0092
dlPFC modulation by inhibitory theta-tACS
(Z-scored BOLD dose-response: tACS > sham)
B
dlPFC: Zmax
STAI trait anxiety
(Z-scored)
dlPFC modulation
(tACS > sham; Z-scored)
C
congruent
incongruent
tACS > sham
(error rates, %)
anti-phase
in-phase
tACS-phase x congruency
D
in-phase tACS
Z-value
-4.5
-2.3
y = -8
x = 17
congruency
(incongruent > congruent)
bilateral amygdala activation
(parameter estimates, a.u.)
tACS-phase x congruency

736

737 ***Table 1. Significant congruency-related whole-brain BOLD activation clusters.***

| contrast | # | Harvard-Oxford structural atlas **brain region** | **cluster size** voxels | **MNI peak coordinates** x | y | z | **max. *Z*-value** | **corrected *p*** |
|---|---|---|---|---|---|---|---|---|
| *incongruent > congruent* | 1 | precuneus,<br>middle temporal gyrus,<br>supramarginal gyrus,<br>angular gyrus,<br>posterior cingulate gyrus,<br>cuneal cortex,<br>lateral occipital cortex,<br>superior parietal lobule,<br>left precentral gyrus,<br>left postcentral gyrus | 7059 | 14 | -70 | 36 | 5.03 | 3.43e-27 |
| | 2 | right frontal pole,<br>right middle frontal gyrus | 1099 | 30 | 36 | 38 | 4.61 | 7.15e-07 |
| | 3 | lingual gyrus,<br>right intracalcarine cortex,<br>right temporal occipital fusiform cortex,<br>right precuneus cortex | 814 | 16 | -74 | -4 | 3.70 | 2.22e-05 |
| | 4 | right paracingulate gyrus,<br>right anterior cingulate gyrus | 326 | 8 | 32 | 28 | 3.71 | 0.027 |
| *congruent > incongruent* | 1 | left temporal pole,<br>left amygdala,<br>left hippocampus,<br>left anterior parahippocampal gyrus,<br>left temporal fusiform cortex | 1376 | -42 | 16 | -36 | 4.86 | 5.96e-08 |
| | 2 | right amygdala,<br>right hippocampus,<br>right anterior parahippocampal gyrus,<br>right temporal pole,<br>right subcallosal cortex,<br>right temporal fusiform cortex | 1028 | 38 | -4 | -20 | 3.98 | 1.61e-06 |
| | 3 | frontal medial cortex,<br>frontal pole | 642 | -8 | 34 | -14 | 3.99 | 0.000217 |
| | 4 | temporal occipital fusiform cortex,<br>inferior temporal gyrus,<br>lateral occipital cortex | 515 | 40 | -42 | -18 | 4.16 | 0.00134 |
| | 5 | right frontal orbital cortex,<br>right frontal pole | 470 | 24 | 28 | -14 | 4.06 | 0.00264 |
| | 6 | left frontal orbital cortex,<br>left frontal pole | 470 | -40 | 28 | -14 | 4.05 | 0.00264 |